INVESTIGATION ON CAM-FOLLOWER LUBRICATED CONTACTS

D. Vela[1], E. Ciulli[1], B. Piccigallo[2], F. Fazzolari[1]

[1] Dipartimento di Ingegneria Meccanica, Nucleare e della Produzione – University of Pisa – Largo Lucio Lazzarino – 56126 Pisa – Italy
dvela@ing.unipi.it, ciulli@ing.unipi.it, francesco_82@hotmail.com
[2] Dipartimento Genio Navale, Accademia Navale – Livorno - Italy
b.piccigallo@ing.unipi.it

ABSTRACT

The cam-follower contact is one of the most complex lubricated non-conformal contact due to its continuous variation of load, speed and geometry. Investigations on new design quantities such as geometry, materials and coatings are important for a reduction of friction losses and wear problems. The complexity of the phenomena occurring in the camshaft systems make experimental verifications very important.

In this work, an already existing versatile experimental apparatus for investigation of non-conformal lubricated contacts, able to measure film thickness using the optical interference method and friction force trough a load cell, has been modified in order to tests cam-follower contacts. Some test have been carried out for investigating the behaviour of some fundamental components of the rig. A theoretical/numerical simulations has been performed to investigate the dynamic behaviour of the system and in order to provide important indications for the interpretation of the experimental results. The programme has been also an important support for the design and of a new apparatus specifically addressed to the cam-follower contact and with increased potentialities capable of more detailed measurement of film thickness and contact forces. The apparatus is able to reproduce a cam-follower mechanism that uses a rocker as a link device between the cam follower set and the valve.

1. INTRODUCTION

The cam-follower contact is one of the most severe of the internal combustion engines. A reduction of friction losses and wear problems of this lubricated non-conformal contact can be very effective for saving energy and materials.
Investigations on new design quantities such as geometry, materials and coatings can be done using real engines or by numerical simulation of the system. The first solution is very expensive and time-consuming, while the second one is very complex. In fact, the cam-follower contact undergoes continuous variation of load, speed and geometry, and dynamic effects of the whole system play an important role. The complexity of the phenomena occurring in the camshaft systems make experimental verifications necessary for a better understanding of what occurs inside a cam-follower contact, but it is very difficult to perform. Friction, film thickness and wear are the most important quantities to be investigated.

In literature, different techniques and methods can be found, such as pin-on-disc apparatus, disc machines, instrumented valve-train set of engines.
Some friction measurements using a cam-follower system are reported in [1-9]. The total friction torque is generally measured and all parasitic losses of the apparatus must be calculated in order to evaluate friction losses in the cam-follower contact. A modified version of the apparatus that allows the follower rotation and the measurement of its frequency is shown in [3]. An apparatus with three load cells that allows the direct measurement of the contact force components is used in [10].
Attempts to measure oil film thickness with a capacitance transducer are made in [11], while electrical resistivity is used in [12]. Film thickness and temperature measurements are performed with thin film micro transducers in [13]. Friction measurements and some first attempts of film thickness and shape evaluation using optical interferometry are reported in [14].
Not many experimental studies on cam-follower contacts have been carried out during the recent years, especially for film thickness measurements. Most studies are addressed to friction and wear measurements for investigating the influence of lubricant additives and surface coatings, finish and texture [15-20].
Optical interferometry has proven the most powerful and detailed method for measuring film thickness and shape, but the continuous variation of the working conditions and therefore of the interference images during running of a cam has made image recording critical till the today availability of high speed cameras. Attempts of using optical interferometry for investigating non-conformal lubricated contacts under transient conditions are reported in [21-26].
There are some experimental problems related with the use of experimental apparata for simulation of the real contacts.
In the lubrication analysis of a cam and follower, the prediction of film thickness and friction requires a precise knowledge of the surface velocities and of the motion of the contact point. In order to validate the predictive models, in the case of direct-action cam and bucket follower, it is common to restrain the bucket follower rotation. In this way the kinematics can be more easily defined. However, in practice the follower is often free to rotate in order to increase durability. Indeed, in many situations an offset between the centre-lines of the cam and follower is introduced to promote the rotation.
A realistic representation and consideration of all factors that join in the valve train is not possible, hence the experimental apparata used to evaluate friction and its non desired effect, the wear, try to simulate the real operating condition under controlled lab-environment. One model of these systems is shown in [27].
Another limitation of most experimental works is that only variable speed conditions are simulated, while the geometry and load variations, also typical of a cam-follower contact, can not be realised with the experimental rigs used, as ball on disk.
Deeper and less time-consuming experimental investigations can be performed with specific test rigs for cam-follower simulation able to measure particularly two very important quantities of a lubricated contact: the friction force and the film thickness.
In this work, the experimental apparatus for friction and film thickness measurements used in [22-25] has been adapted for testing cam-follower contacts and verify the simulation programme also used for the design of a new experimental apparatus.

2. RECONFIGURED EXPERIMENTAL APPARATUS

An already existing versatile experimental apparatus for investigation of non-conformal

lubricated contacts, able to measure film thickness using the optical interference method and friction force trough a load cell, has been modified in order to make it possible tests on cam-follower contacts. The apparatus has been used for some preliminary experiments and for testing a simulation programme, based on dynamic equations briefly described in the next section, used for an optimised design of a new experimental apparatus specifically addressed to cam-follower contacts.
The same configuration used in a former study [14] has been used. However, more detailed results are available thanks to the improvements realised since the previous investigation, particularly the use of a data acquisition system and of a high speed camera.
A Schematic drawing of the apparatus is shown in Fig. 1.
The contact is developed between the cam and the plane surface of a disc. A glass disc is used when optical interferometry is employed for film thickness and shape measurements. The friction force is measured trough a load cell (Fig.2) that restrain the rotation of the disc supported by a radio-axial gas bearing. The normal load is applied through dead weights thanks to a lever system with a gas bearing as a fulcrum.

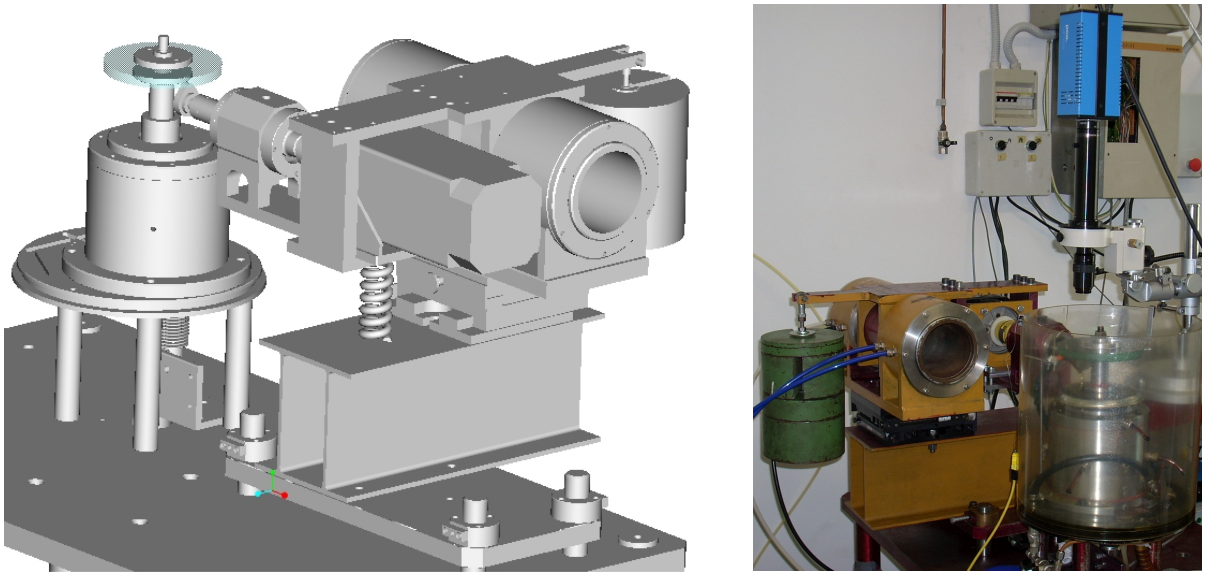

a b

Fig. 1 - Experimental apparatus for friction and film thickness measurements in the configuration for cam investigations. Schematic drawing (a) and picture of the apparatus (b).

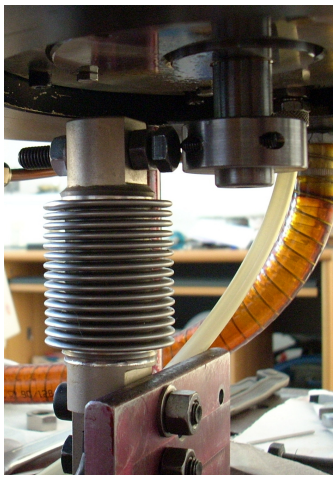

Fig. 2 – Detail of the load cell used for measuring the friction force.

Dynamic aspects can play an important role for this system that can be used to simulate valve train system as well as gear teeth contacts. Therefore, a dynamic simulations of the apparatus has been performed which includes a detailed description of the cam follower contact.

3. DYNAMIC SIMULATION

A programme for the dynamic simulation of all moving parts of the apparatus has been developed in the Matlab-Simulink® environment. The system has been schematized as shown in Fig. 3. The dynamic equations have been obtained by means of a standard Lagrangian approach. The torsional compliance of the flexible joint *g* between the motor 1 and specimen's shaft 2 has been also included in the model as well as the presence of two unbalancing masses *m* on both sides of the joint due to the presence of the tabs. The rotation of the arm 3, whose centre of mass is located in G, is related to the vertical displacement of the cam axis *y* that is also related to the cam rotation angle α.

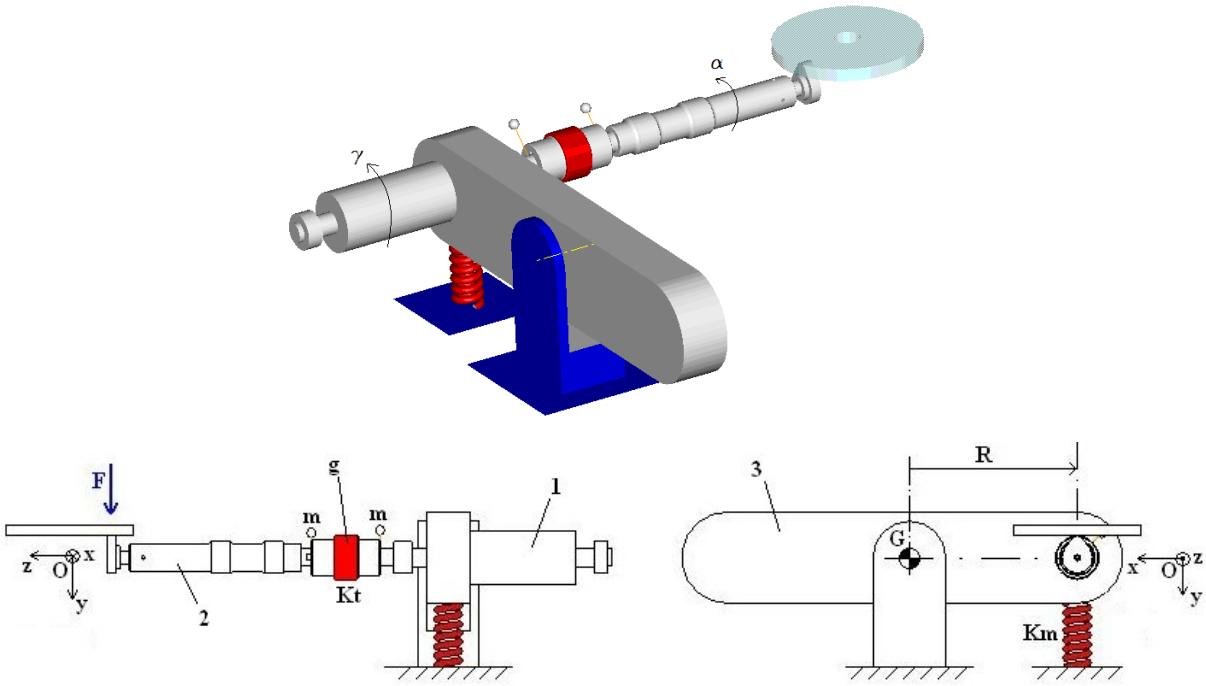

Fig. 3 - Dynamic scheme of the experimental apparatus.

The resolutive equation obtained for the angular acceleration of the cam is:

$$\ddot{\alpha}=\frac{K_t(\gamma-\alpha)-M_r-f\left[y(\alpha)+R_b\right]\{\frac{J_G}{R^2}y''(\alpha)\dot{\alpha}^2+K_m\left[y(\alpha)+y_{st}\right]+m\,e_m\dot{\gamma}^2\cos(\dot{\gamma}t)+m\,e_m\dot{\alpha}^2\cos(\dot{\alpha}t)\}}{J_2+me_m^2+\frac{J_g}{2}+f\frac{J_G}{R^2}y'(\alpha)\left[y(\alpha)+R_b\right]}$$

where, K_t is the stiffness of the torsional joint, $\gamma,\dot{\gamma}$ the angular position and velocity of the motor's shaft (known quantities), $\alpha,\dot{\alpha}$ the angular position and velocity of the cam, M_r the rolling bearing frictional torque, f the friction coefficient of the lubricated contact point,

$y(\alpha)$, $y'(\alpha)$, $y''(\alpha)$ the displacement of the contact point along the *y* direction and its first and second derivative respect to α, R_b the cam base radius, R the distance between the test article shaft rotation axis and the fulcrum G, K_m and y_{st} the spring stiffness and possible static deflection (for *y*=0), *m* and e_m the unbalanced masses and their eccentricity, t the time, J_2 , J_g and J_G the mass inertia moments of test article shaft 2 (including the cam and all related rotating masses), of the torsional joint and of the whole system 3 rotating around the fulcrum G.
The normal contact force can be then evaluated by the equation:

$$F=\frac{J_G}{R^2}\left[y''(\alpha)\dot{\alpha}^2+y'(\alpha)\ddot{\alpha}\right]+K_m\left[y(\alpha)+y_{\mathrm{st}}\right]+m\,e_m\dot{\gamma}^2\cos(\dot{\gamma}\,t)+m\,e_m\dot{\alpha}^2\cos(\dot{\alpha}\,t)$$

The torque due to the friction force in the contact is included by using the formula for the estimation of the friction coefficient *f* reported in [28].
Some details of the kinematic relationships used are reported in the appendix.

4. TESTS WITH A CIRCULAR CAM

Some preliminary experiments have been made using an eccentric circular cam in order to validate the simulation programme and to set up the experimental procedure and some new components.
The cam used, made of steel, has a spherical surface with radius *r*=20 mm and a root mean square roughness R_q=0.15 μm; the eccentricity is *e*=4 mm.
A glass disc has been used as a counterface for recording interference images. A load of 20 N has been applied through dead weights.
Tests have been carried at 6, 15, 36 and 60 rpm at a room temperature of about 30°C. A SAE 5W-40 has been used as a lubricant, whose viscosity at the test temperature is about 0.13 Pas.
The tests have been carried out both without the spring shown in Fig. 3 and with one with stiffness 11.25 N/mm not loaded at the reference cam rotation angle θ=0° corresponding to the point contact on the base circle (see Fig. A2).
The calculated contact point displacement *x* and the vertical displacement *s* are shown in Fig. 4a. It is worth noting that *s* usually corresponds to the movement of the follower while it corresponds to the movement of the cam axis in the investigated conditions. The contact point velocity formula $\dot{x}$ and the entraining velocity *u* are shown in Fig. 4b (the data refers to the 6 rpm case). It is evident that formula $\dot{x}$ changes its direction every 180° while *u* has always the same direction.
The calculated normal contact force is shown for two different rotational speeds of the cam in Fig. 5 for the case without (Fig. 5a) and with spring (Fig. 5b). The increasing influence of the dynamic effects as speed increases is particularly evident from Fig. 5a. The presence of the spring increases the force and shifts the extreme values of 180°.
Force data have been recorded every rotation angle degree for three cycles at every rotational speed tested. Accordingly, the frequency of the high speed camera has been adjusted in order to record an image for every angular degree.
The actual friction force is calculated from the values measured by the load cell taking into account the distances between the disc axis, the load cell axis and the contacts points between cam and disc.

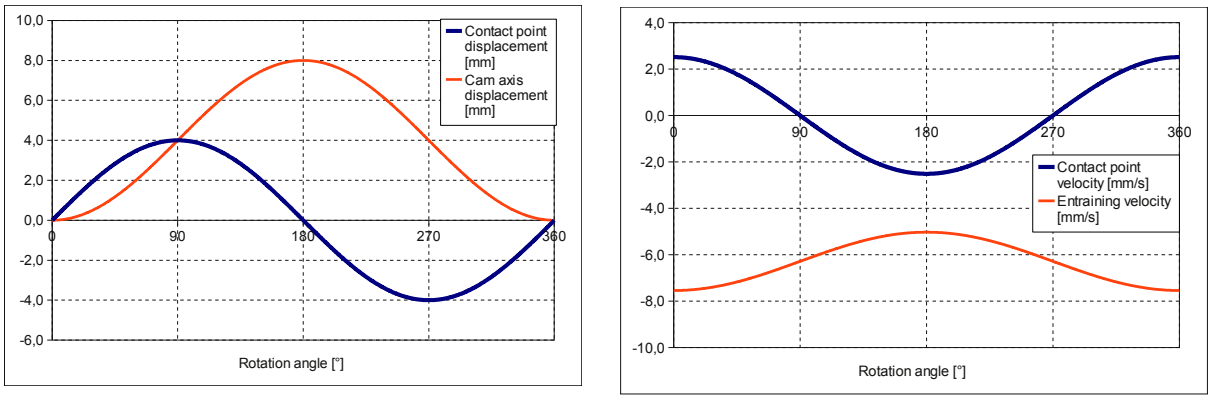

a b

Fig. 4 – Trends of displacements (a) and velocities (6 rpm) (b)

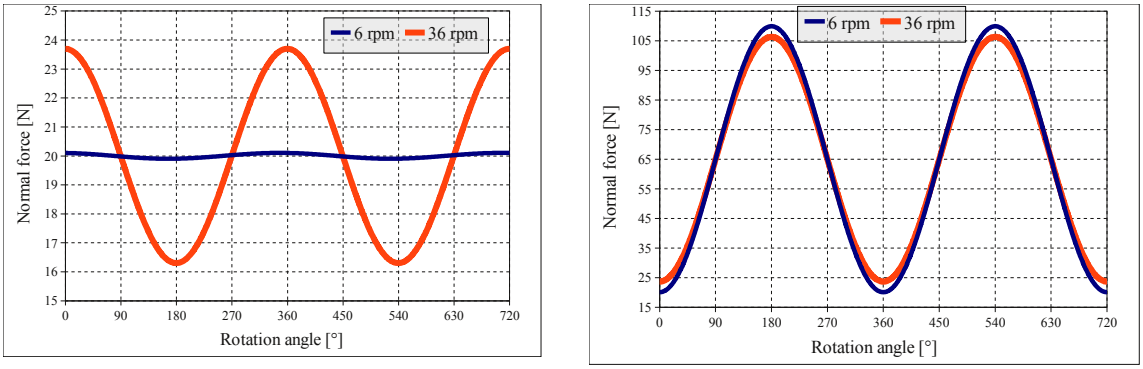

a b

Fig. 5 – Calculated normal contact load at 6 and 36 rpm without (a) and with (b) spring.

Examples of friction force trends obtained from tests at 15 rpm without and with spring are shown in Fig. 6. The evident fluctuations of the data can be related to electrical noise as well as to the presence of wear on the cam surface described later in this paragraph. For an easier comparison among results, the data have been filtered using the same methodology reported in [29].

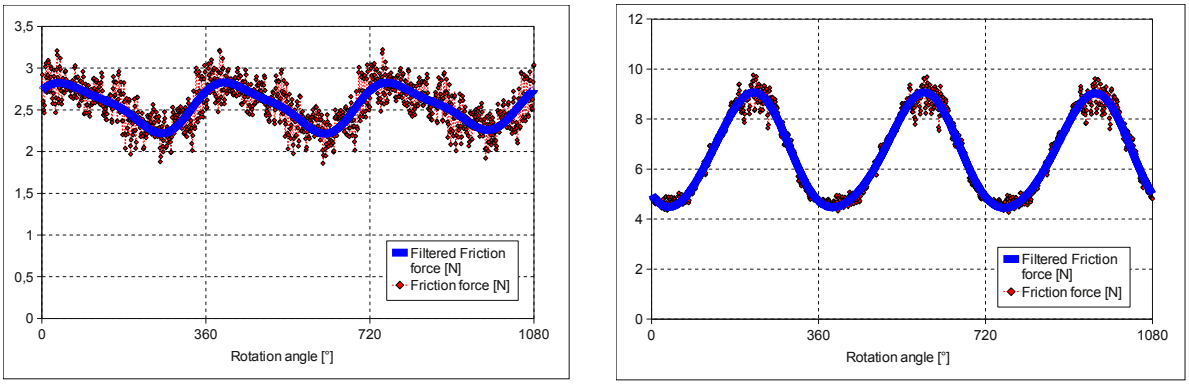

a b

Fig. 6 – Measured friction force and corresponding filtered trends at 15 rpm without (a) and with (b) spring.

Filtered trends obtained from the recorded data at three different velocities without spring are shown in Fig. 7. Two cycles for each case are reported starting conventionally at 0° with the minimum value. However, it is worth mentioning that the correspondence between the friction value and the angular position was not an available information for the tests performed. Recording of data starts when the imposed rotational speed is reached, which can occur at different angular position, and there is no sensors that can detect the angular position in the used experimental apparatus. This drawback will be overcome with the new rig introduced in the next paragraph. In addition, it is not easy to put in relation the friction force and the angular position from theoretical considerations because the transient conditions that occur in this kind of contact. The variations of load and speed shown in Fig. 4 and Fig. 5 produce a time shift between film thickness, friction force, load and speed, as reported for instance in [26].

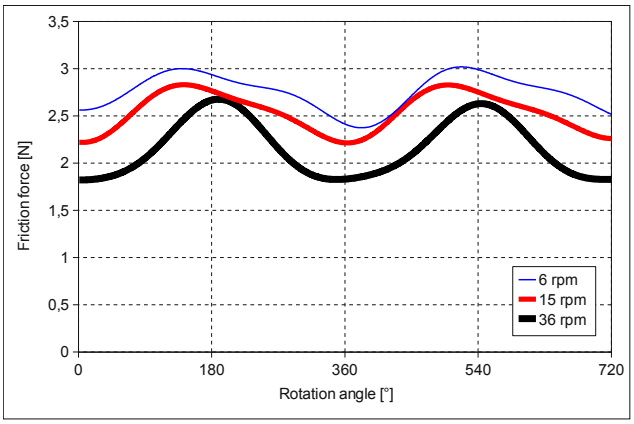

Fig. 7 – Filtered friction force trends for three different velocities in tests without spring.

Despite this drawback, an average reduction of the friction force by increasing the speed is evident from Fig. 7. This indicates that tests have been carried out meanly under mixed lubrication conditions, as confirmed by the values of minimum film thickness h_m and Λ (the ratio between the minimum film thickness and the equivalent root mean square roughness of the two contacting bodies) reported in Tab. 1. The values have been calculated with one of the classical formulas for isothermal steady state conditions using 20 N load and the minimum and maximum values of the entraining velocity during a cycle.

Velocity [rpm]	h_m [µm]	Λ
6	0.014-0.018	0.09-0.12
15	0.026-0.034	0.17-0.23
36	0.047-0.062	0.31-0.41
60	0.067-0.088	0.44-0.58

Tab. 1 – Minimum film thickness and lambda ratio for the minimum and maximum entraining velocity during a complete cam rotation for the four velocities tested.

The mixed (and in certain cases also boundary) lubrication conditions are also confirmed by a rough estimation of the friction coefficient (the mean values are ranging from 0.1 to 0.15) and by the recorded interference images.
An example of images recorded during a complete rotation of the cam is shown in Fig. 8, where some interference images recorded every 45° are put together in order to give a better idea of the whole movement of the contact point. The distance between the interferograms is not constant because the variation of the contact point velocity, that reaches its maximum absolute value at 0° and 180° (as shown in Fig. 4b). The highest entraining velocity is at 0°, while the lowest at 180°. The lowest entraining velocity together with the highest normal load produced the most severe conditions around 180° and some wear of the cam occurred as evident from the picture of Fig. 9.

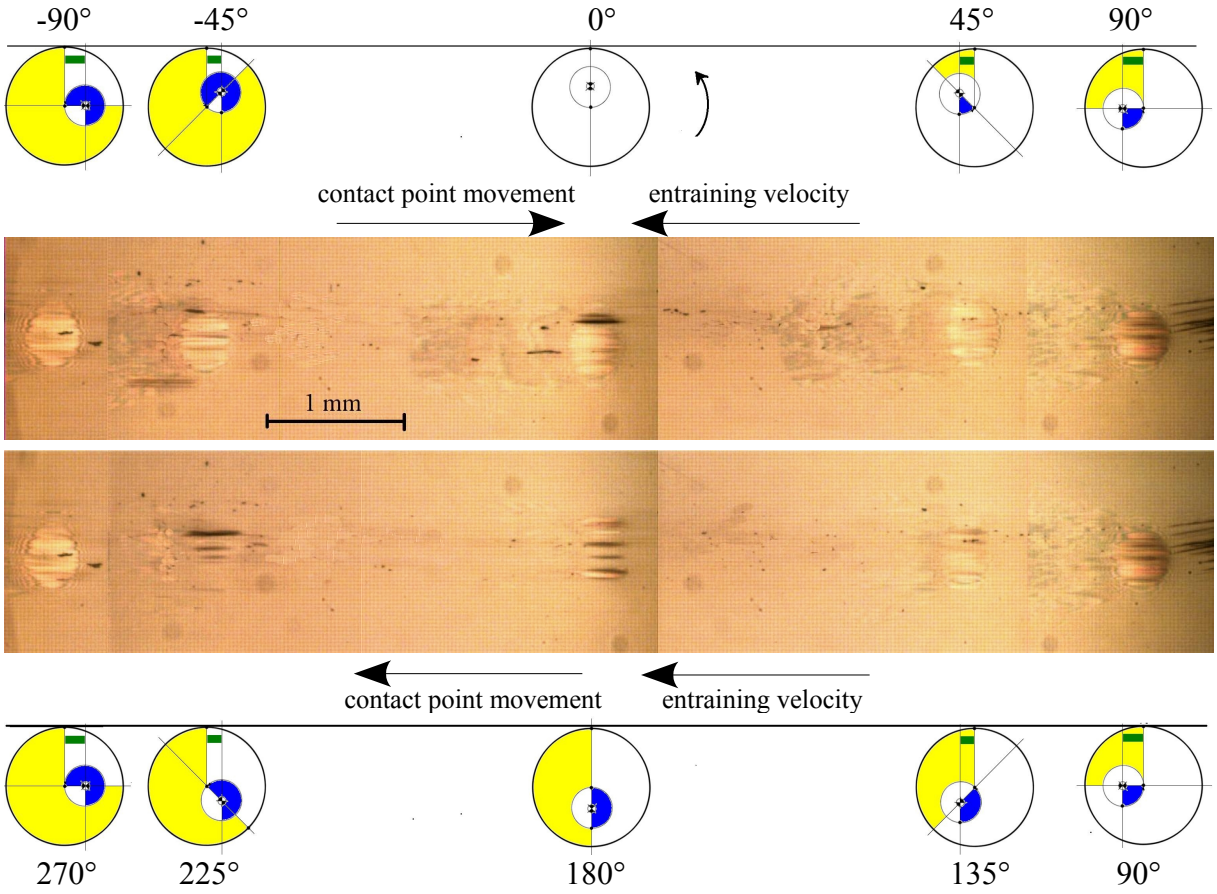

Fig. 8 – Collage of interference images recorded every 45° during a complete rotation of the cam at 36 rpm and schematic drawing of the contact point movement.

Fig. 9 – After tests picture of the specimen. Wear marks around 180° angular position.

An evaluation of the film thickness from the interference images was not one of the aim of this work. However, a preliminary analysis of the recorded images has been done and put in evidence the capability of the methodology used to detect some interesting aspects, such as the presence of a cavitated region of increasing magnitude by increasing the velocity (Fig. 10) and the increasing of the Hertzian zone with the load (Fig. 11).

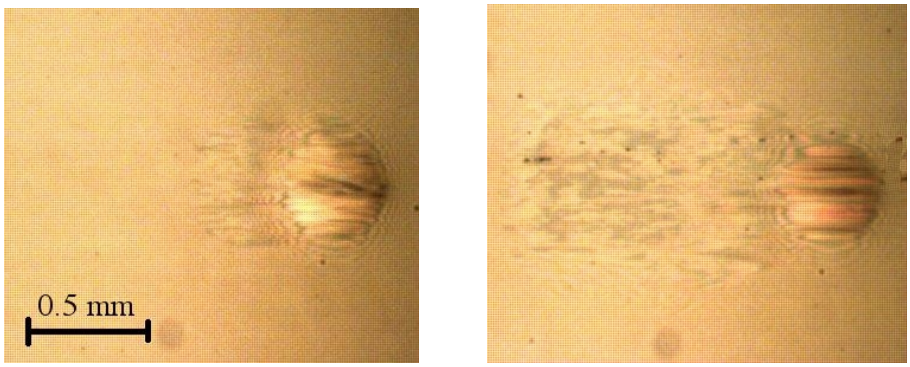

a b

Fig. 10 – Velocity effect: interference images recorded at 90° at 6 (a) and 36 (b) rpm.

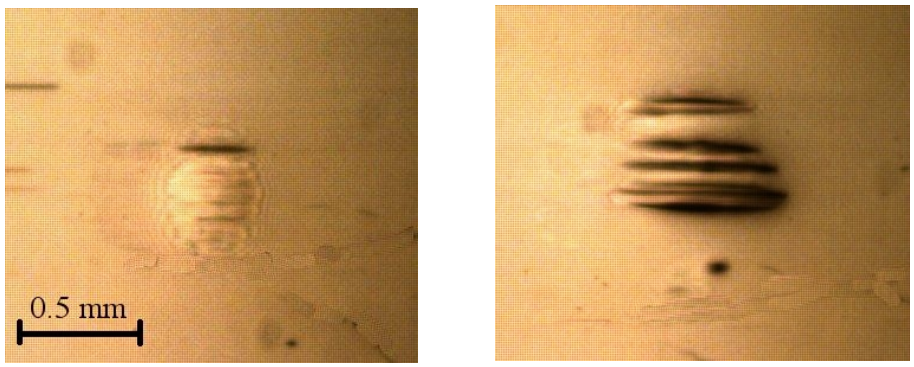

a b

Fig. 11 – Load effect: interference images recorded in presence of spring at 6 rpm at 0° (a) and 180° (b).

5. FUNDAMENTAL ASPECTS OF THE NEW APPARATUS

By using the experience made with the existing experimental apparatus and the dynamic simulation programme, a new test rig with increased potentialities has been designed. This is specifically addressed to the cam-follower contacts and its set up is currently under way. Full details of the rig will be reported in a specific work. Its main aspects are briefly described here.

The fundamental quantities to be measured are film thickness and contact force. The film thickness and shape is estimated by interferometric method using a new microscope, employed for the first time in the tests carried out with the existing apparatus, connected with the high-speed camera. A system of annular quartz load cells is employed for the measurement of every component of the contact force.

Advanced versions of the simulation programme have been used for the design of the test rig. The dynamic behaviour of several design versions have been investigated [30], [31]. The final

version of the apparatus is able to reproduce different cam-follower mechanisms using different configurations. The basic configuration is shown in Fig. 12. The system consists of two main parts: the power transmission unit and the measurement unit. The first one include a rocker arm where the cam shaft is installed. The cam is driven by an epicycloidal gear system moved by an electric motor connected through a flexible joint on the same axis of the fulcrum of the arm. An absolute encoder positioned after the elastic joint allows the direct measurement of the angular position and velocity of the cam. The load is applied through a adjustable loading spring system. The contact between the cam and the follower occurs in the measurement unit. This part can be arranged in several configurations including the ones with moving follower. In the basic version, shown in more detail in Fig. 13, the follower is not moving and optical interference is possible when the follower is made of glass. The microscope can be moved by a computer controlled xyz positioner, also shown in Fig. 12.

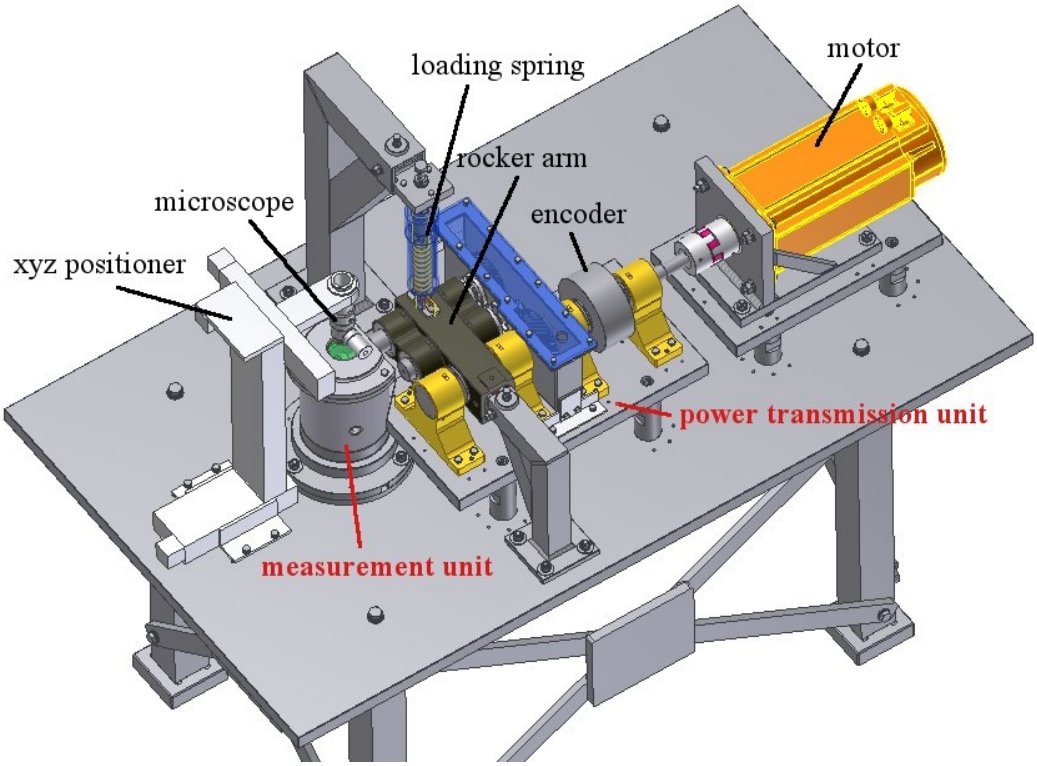

Fig. 12 - Three-dimensional view of the new experimental apparatus.

Nine annular load cells are used mounted together in groups of three composed by two tangential cells and one for normal load. The position of the cells is indicated in Fig. 13, where also the ceramic blocks for thermal insulation of the zone with the lubricant are visible. An important aspect of the apparatus is its versatility. By changing the measurement group, the apparatus is able to reproduce a cam-follower mechanism in most configurations that are used in engine valve trains.

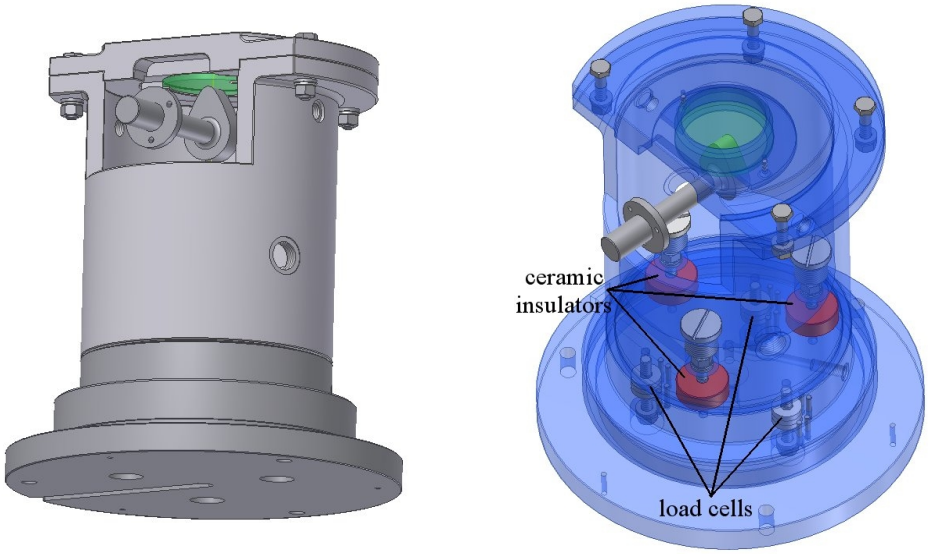

a b

Fig. 13 – Measurement unit (a) and details of some its internal parts (b).

6. CONCLUSIONS

The complexity of the phenomena occurring in the camshaft systems make experimental verifications very important. However, the simulation of the real contacts and the measurements of friction force and film thickness are not easy. Numerical simulations can furnish important indications both for interpretation of the experimental results and the design procedures.

An existing versatile apparatus has been reconfigured for simulation of the cam-follower contact. It has been used for some preliminary experiments with a spherical circular cam for testing a purposely developed programme for the dynamic simulation of the system. Friction force and interference images of the lubricated contact have been recorded. The tests have been performed also in order to set up and verify the functionality of some new acquired components that will be used with a new experimental apparatus. This has been specifically designed for the cam-follower contacts and presents increased potentialities as the capability of more detailed measurement of film thickness and contact forces. The design of the new apparatus, whose set up is currently under way, has been optimised on the basis of the experience made with the existing test rig and using purposely modified versions of the dynamic simulation programme.

The experimental tests performed with the existing apparatus have confirmed the possibility to use optical interferometry for the measurement of the film thickness also for the cam-follower contact that presents the problem of a moving contact point. The use of a computer controlled xyz positioner for the movement of the microscope with the connected high-speed camera will allow deeper investigations with the new apparatus.

The investigations, made under transient conditions of load and speed, have also put in evidence the importance of recording all data at the same time and the necessity to have additional information such as the angular position of the cam and the normal contact load. The synchronism among the recorded data and images will be realised by triggering the high speed camera and the data acquisition system. An absolute encoder and a system of nine annular load cells present in the new apparatus allow the direct measurement of angular position and all components of the contact force.

Finally, wear problems have been detected that evidence the importance of a detailed design of experiments for the tests with the new apparatus. Tests order should be decided trying to confine at the end tests conditions with more probable wear problems.

ACKNOWLEDGEMENT
Authors would like to thank Eng. Sergio Segreto for the development of the first simulation programme.

REFERENCES

[1] Dowson, D., Harrison, P. and Taylor, C.M., "The lubrication of automotive cams and followers", in Proc. 12th Leeds-Lyon Symposium on Tribology, Butterworths, Oxford, 305-322 (1986).
[2] Taylor C.M., Valve Train Lubrication Analysis. Proceedings of the 17th Leeds-Lyon Symposium on Tribology. Elsevier, Amsterdam, 1992, 159-182.
[3] Taylor C. M., Fluid film lubrication in automobile valve trains. Proc. IMechE, vol 208, Journal of Engineering Tribology, 1994, 221-234.
[4] Taylor C. M., Cam and Followers: Background and Lubrication Analysis. Engine Tribology/CM Taylor Editors, 1993, 159-182.
[5] Dowson D., Taylor C. M., Zhu G., "A transient elastohydrodynamic lubrication analysis of a cam and follower", International Conference on Frontiers of Tribology, UK, 15-17 April 1991.
[6] Xuesong M., Youbai X., A numerical analysis of the non-steady EHL process in high-speed rotating engine cam/tappet pairs. J. Tribology-ASME, Vol. 118, 1996, 637-643.
[7] Kushwaha M., Rahnejat H., Jin Z. M., Valve-train Dynamics: A Simplified Tribo-Elastic-Multi-body Analysis. Proc. Instn. Mech. Engrs., J. Multi-body Dynamics, Part K 214, 2000, 95–110.
[8] Kushwaha M., Rahnejat H., Transient elastohydrodynamic lubrication of finite line conjuction of cam to follower concentrated contact. J. Physics D: Applied Physics, Vol. 35, 2002, 2872-2890.
[9] Dowson, D., Taylor, C.M. and Zhu, G., "A transient EHL analyses of a cam and follower", J. Phys. Appl. Phys., 25, 313-320 (1992).
[10] Bair, S., Griffioen, J.A. and Winer, W.O., "The tribological behavior of an automotive cam and flat lifter system", Transaction of the ASME, Journal of Tribology, 108, 478-486 (1986).
[11] Hamilton, G.M., "The hydrodynamic of a cam follower", Tribology International, 13, 113-119 (1980).
[12] Dowson, D., Harrison, P., Taylor, C.M. and Zhu, G., "Experimental observation of lubricant film state between a cam and bucket follower using the electrical resistivity technique", in Proc. Japan International Tribology Conference, Nagoya, Japan, 119-124 (1990).
[13] van Leeuwen, H., Meijer, H. and Schouten, M., "Elastohydrodynamic film thickness and temperature measurements in dynamically loaded concentrated contacts: eccentric cam-flat follower", in Proc. 13th Leeds-Lyon Symposium on Tribology, Elsevier, Amsterdam, 611-625 (1987).
[14] Bassani, R., Ciulli, E. and Forte, P., "Experiences of elastohydrodynamics on spheres and cams", in Proc. X AIMETA General Congress, Pisa 2-5 October 1990, Edizioni ETS, Pisa, Vol. 2, 427-432 (1990) (in Italian).

[15] Willermet, P.A., Pieprzak, J.M., Dailey, D.P., Carter, R.O., Lindsay, N.E., Haack, L.P. and deVries, J.E., "The Composition of Surface Layers Formed in a Lubricated Cam/Tappet Contact", Transaction of the ASME, Journal of Tribology, 113, 38-47 (1991).
[16] Soejima, M., Ejima, Y., Wakuri, Y. and Kitahara, T., "Improvement of lubrication for cam and follower", Tribology Transactions, 42, 4, 755-762 (1999).
[17] Gangopadhyay, A., Soltis, E. and Johnson, M.D., "Valvetrain friction and wear: influence of surface engineering and lubricants", Proc. Instn. Mech. Engrs., Journal of Engineering Tribology, 218, 147-156 (2004).
[18] Kano, M., "Super low friction of DLC applied to engine cam follower lubricated with ester-containing oil", Tribology International, 39, 1682-1685 (2006).
[19] Lewis, R. and Dwyer-Joyce, R.S., "Wear of diesel engine inlet valves and seat inserts", Proc. Instn. Mech. Engrs., Journal Automobile Engineering, 216, 205-216 (2002).
[20] Hua D. Y., Farhang K., Seitzman L. E., A multi-scale system analysis and verification for improved contact fatigue life cycle of a cam-roller system. J. Tribology-ASME, Vol. 129, 2007, 321-25.
[21] Glovnea, R.P. and Spikes, H.A., "The influence of cam-follower motion on elastohydrodynamic film thickness", in Proc. 27th Leeds-Lyon Symposium on Tribology, Elsevier, Amsterdam, 485-493 (2001).
[22] Bassani, R., Ciulli, E., Stadler, K. and Carli, M., "Lubricated non-conformal contacts under steady-state and transient conditions", in Proc. XVII AIMETA General Congress, Firenze, 11-15 September 2005, 11 pages, on CD (2005).
[23] Bassani, R., Ciulli, E., Carli, M. and Stadler, K., "Experimental investigation of Transient and Thermal Effects on Lubricated non-conformal Contacts", Tribotest, 13, 183-194 (2007).
[24] Ciulli, E., Draexl, T. and Stadler, K., "Film Thickness Analysis for EHL Contacts under Steady-State and Transient Conditions by Automatic Digital Image Processing", Advances in Tribology, Vol. 2008, Article ID 25187, 16 pages, 2008. doi:10.1155/2008/25187, http://www.hindawi.com/journals/at/volume-2008/, ISSN: 1687-5915, e-ISSN: 1687-5923, doi:10.1155/AT (2008).
[25] Ciulli, E., Stadler, K. and Draexl, T., "The influence of the slide to roll ratio on the friction coefficient and film thickness of EHD point contacts under steady state and transient conditions", Tribology International, 42 (4), 526-534 (2009).
[26] Ciulli, E., "Non-steady state non-conformal contacts: friction and film thickness studies", Meccanica, 44, 409-425 (2009).
[27] Lindhom P. and Svahn F., "Study of thickness of sputtered-carbon coating for low friction valve lifters", Wear, 261, 241-250 (2006).
[28] Ciulli, E., Bartilotta, I., Polacco, A., Manconi, S., Vela, D., Guerrieri Paleotti, F.S., "A Model for Scuffing Prediction", Journal of Mechanical Engineering, 56(2010), ISSN 0039-2480, 231-238 (2010).
[29] Ciulli, E., "Time and frequency domain analysis of experimental EHL transient conditions data", Proceedings of the 11th Symposium on Tribology, Tromsø-Harstad-Hurtigruten, Norway, June 2004, 575-584 (2004).
[30] Vela, D., Ciulli, E. and Piccigallo, B., "Wear and elastohydrodynamic lubrication studies of cams and followers", Proceedings of ECOTRIB 2009 – 2nd European Conference on Tribology, Pisa, Italy, June 7-10, 2009, Edizioni ETS, Pisa, ISBN 978-884672426-7, Vol.2, 957-962 (2009).
[31] Ciulli, E., Piccigallo, B., Vela, D., "Experimental study of engine cam-followers", XIX Congresso AIMETA, Ancona, 14-17 Settembre 2009, Aras Edizioni, Fano, 2009, ISBN 978-88-96378-08-3, 10p., on CD (2009).

APPENDIX

Kinematic formulas

The movement of the cam axis is related to the rotation of the cam and therefore to its shape. By using a reference coordinate system with the origin in the cam axis (Fig. A1), the coordinates of the contact point can be put in relation to the angular position α of the cam.

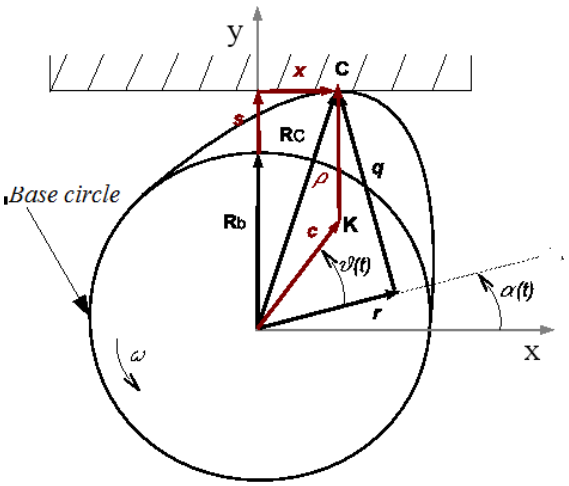

Fig. A1 – Geometric quantities of the cam-follower contact.

With reference to Fig. A1, the position of cam-follower contact point can be expressed by the equivalent formulas:

$$\vec{R}_C = x\,\hat{i} + (R_b + s)\,\hat{j} \quad \text{and} \quad \vec{R}_C = \vec{c} + \rho\,\hat{j}$$

where $\hat{i}$ and $\hat{j}$ are the unit vectors of the x and y axes respectively.
By equating the two vectorial expressions, two scalar equation can be obtained:

$$x = c\cos(\alpha + \vartheta) \quad \text{and} \quad y = R_b + s = c\sin(\alpha + \vartheta) + \rho$$

and by derivation respect to a the variable α:

$$x' = \frac{dx}{d\alpha} = -c\sin(\alpha + \vartheta) \quad \text{and} \quad y' = \frac{dy}{d\alpha} = c\cos(\alpha + \vartheta)$$

It is easy to verify that

$$s' = \frac{ds}{d\alpha} = y' = x$$

and

$$s'' = \frac{d^2 s}{d\alpha^2} = y'' = x'$$

As well known, the physical points of the two bodies in contact in C have the same velocity in the y direction but generally different ones in the x direction. Along the x direction, the velocity of the cam's point is:

$$v = -y\frac{d\alpha}{dt} = -y\omega$$

while the one of the contacting body is zero. The contact point is moving with the velocity:

$$\dot{x} = \frac{dx}{dt} = \frac{dx}{d\alpha}\frac{d\alpha}{dt} = x'\omega = s''\omega$$

The entraining velocity u can be calculated as the mean velocity referred to the contact point:

$$u = \frac{(v-\dot{x})+(0-\dot{x})}{2} = -\frac{(y+2s'')\omega}{2} = -\frac{(R_b+s+2s'')\omega}{2}$$

For every cam, the law $y(\alpha)$ is known, so that all the above quantities can be calculated for every angular velocity ω.

For a circular cam of radius r and eccentricity e (Fig. A2), it is easy to find the relations reported below (the angle θ, has been used as cam rotation angle, with θ=0 corresponding to the minimum distance between the cam axis and the contact point, when it is on the base circle of radius R_b=r-e).

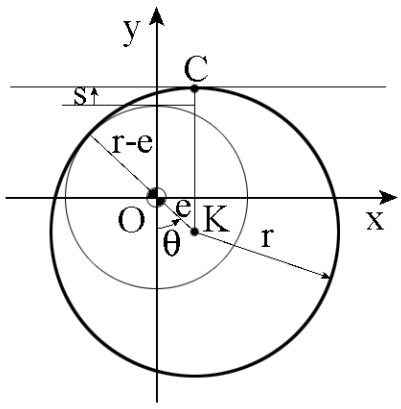

Fig. A2 – Geometric quantities for an eccentric circular cam.

$$x = e\sin(\theta) \quad \text{and} \quad y = R_b + s = R_b + e\left[1-\cos(\theta)\right]$$

$$\dot{x} = e\omega\cos(\theta)$$

$$u = -\frac{\{R_b + e\left[1+\cos(\theta)\right]\}\omega}{2}$$